Molecular Biology of the Cell
Vol. 10, 1001–1017, April 1999

The Tail of a Yeast Class V Myosin, Myo2p, Functions as a Localization Domain

Samara L. Reck-Peterson,*† Peter J. Novick,* and Mark S. Mooseker*‡§

*Department of Cell Biology and ‡Department of Pathology, Yale University School of Medicine, New Haven, Connecticut 06520; and §Department of Molecular, Cellular Developmental Biology, Yale University, New Haven, Connecticut 06520

Submitted August 27, 1998; Accepted February 1, 1999
Monitoring Editor: David Drubin

Myo2p is a yeast class V myosin that functions in membrane trafficking. To investigate the function of the carboxyl-terminal-tail domain of Myo2p, we have overexpressed this domain behind the regulatable *GAL1* promoter (*MYO2DN*). Overexpression of the tail domain of Myo2p results in a dominant–negative phenotype that is phenotypically similar to a temperature-sensitive allele of *myo2, myo2–66*. The tail domain of Myo2p is sufficient for localization at low- expression levels and causes mislocalization of the endogenous Myo2p from sites of polarized cell growth. Subcellular fractionation of polarized, mechanically lysed yeast cells reveals that Myo2p is present predominantly in a 100,000 × *g* pellet. The Myo2p in this pellet is not solubilized by Mg^{++}-ATP or Triton X-100, but is solubilized by high salt. Tail overexpression does not disrupt this fractionation pattern, nor do mutations in *sec4, sec3, sec9, cdc42,* or *myo2*. These results show that overexpression of the tail domain of Myo2p does not compete with the endogenous Myo2p for assembly into a pelletable structure, but does compete with the endogenous Myo2p for a factor that is necessary for localization to the bud tip.

INTRODUCTION

The myosin superfamily consists of at least 15 distinct classes of presumed actin-based molecular motors. These myosin classes are defined by the presence of a structurally conserved motor domain first characterized for the class II (or conventional) myosins of muscle and nonmuscle cells (Mermall *et al.*, 1998; Probst *et al.*, 1998; Wang *et al.*, 1998). The motor domain of characterized myosins hydrolyzes ATP in the presence of F-actin to create force; all myosins contain the sequences that are predicted to be involved in ATP hydrolysis and actin binding. With one known exception (Heintzelman and Schwartzman, 1997), the motor domain is linked to the C-terminal tail domain by a neck (or regulatory) domain of variable length that contains sites for binding of light chains of the calmodulin superfamily (Mermall *et al.*, 1998). The tail domain is the most divergent domain among the different myosin classes. The tail domains of many unconventional myosins contain protein motifs known to function in signal transduction, membrane binding, or protein–protein interactions (reviewed in Mermall *et al.*, 1998). Although the tail domain is thought to be important for localization and cargo binding, its function remains largely unknown for most myosins.

Analysis of mutations of class V myosins in yeast, mouse, and man has revealed that class V myosins, among other functions, are involved in membrane trafficking. Yeast that have a temperature-sensitive mutation within the motor domain of *MYO2*, a class V myosin, accumulate 80- to 100-nm cytoplasmic vesicles (Johnston *et al.*, 1991; Govindan *et al.*, 1995). *dilute* mice, which have mutations in Myosin Va, fail to properly localize smooth endoplasmic reticulum in neurons and pigment granules in melanocytes (Mercer *et al.*, 1991; Provance *et al.*, 1996; Takagishi *et al.*, 1996). In humans, Myosin 5a has been identified as the target gene for Griscelli syndrome, which is characterized by severe immunodeficiency and partial albinism (Griscelli *et al.*, 1978; Pastural *et al.*, 1997). The basis for this immunodeficiency is unknown, but the albinism

† Corresponding author. E-mail address: reckpesl@biomed.med.yale.edu.

is likely to be a result of improper transport of pigment-containing organelles, as is the case in the *dilute* mouse. These genetic data suggest that class V myosins are involved either directly or indirectly in organelle transport.

To further support the idea that class V myosins may be involved in vesicle trafficking, biochemical and immunocytochemistry studies have shown that class V myosins both colocalize and cofractionate with cytoplasmic organelles (Espreafico *et al.*, 1992; Evans *et al.*, 1997, 1998; Nascimento *et al.*, 1997; Prekeris and Terrian, 1997; Rogers and Gelfand, 1998). For example, immunoelectron microscopy experiments have shown that myosin V labels melanosomes in melanocytes and vesicles enriched for synaptic vesicle markers in neurons (Nascimento *et al.*, 1997; Prekeris and Terrian, 1997; Wu *et al.*, 1997; Evans *et al.*, 1998). These myosin V-associated organelles from neurons or melanocytes are capable of supporting actin-based motility in an in-vitro- motility assay, further evidence that myosin V may function as an organelle motor (Evans *et al.*, 1998; Rogers and Gelfand, 1998).

The yeast *Saccharomyces cerevisiae* has five myosin genes, including two class V myosins, *MYO2* and *MYO4* (Brown, 1997). *MYO4*, a nonessential gene, is required for mating type switching in yeast; specifically, *MYO4* is required for proper localization of *ASH1* mRNA (Haarer *et al.*, 1994; Bobala *et al.*, 1996; Jansen *et al.*, 1996; Long *et al.*, 1997; Takizawa *et al.*, 1997). *MYO2* is an essential gene, suggesting that *MYO2* and *MYO4* have distinct and nonoverlapping functions. The temperature-sensitive allele of *MYO2*, myo2-*66*, arrests as large unbudded cells that have a disorganized actin cytoskeleton, mislocalize chitin, and accumulate vesicles in the mother cell (Johnston *et al.*, 1991; Govindan *et al.*, 1995). Given this phenotype, it has been proposed that Myo2p functions to transport some class of vesicles from the mother cell to the daughter cell along actin filaments during budding (Johnston *et al.*, 1991; Govindan *et al.*, 1995).

The identity of the vesicles that accumulate in *myo2–66* remains unknown, although epistasis analysis suggests that these vesicles are post-Golgi in origin (Govindan *et al.*, 1995). No transport defects have been detected for the secretion markers, invertase and α-factor, protein traffic to the vacuole, or endocytosis in *myo2–66* cells (Govindan *et al.*, 1995). A defect in the secretion of the cell-surface protein, a-agglutinin, has been reported (Liu and Bretscher, 1992). As *myo2–66* cells exhibit defects in vacuolar inheritance, a separate process from vacuolar protein sorting, the vesicles that accumulate in *myo2–66* cells could represent fragmented vacuole (Hill *et al.*, 1996; Wang *et al.*, 1996). However, vacuolar inheritance is a nonessential process whereas *MYO2* is an essential gene, suggesting that *MYO2* may be involved in trafficking other organelle populations. For instance, Myo2p could be involved in localizing organelles referred to as chitosomes, because Chs3p, an enzyme involved in chitin synthesis that is present on chitosomes, is mislocalized in *myo2–66* (Chuang and Schekman, 1996; Santos and Snyder, 1997). Sec4p, a member of the rab family of guanosine triphosphatases that functions in post-Golgi vesicle trafficking, is also mislocalized in *myo2–66* (Walch-Solimena *et al.*, 1997). As *myo2* and *sec4* mutants do not have the same trafficking defects, it is possible that Myo2p is required for polarized transport of vesicles, but does not participate in vesicle fusion, as does Sec4p.

Myo2p is localized to regions of polarized cell growth (Lillie and Brown, 1994). *myo2–66* cells grown at the permissive temperature demonstrate reduced polarized Myo2p staining, whereas localization to regions of polarized cell growth is abolished at the restrictive temperature (Lillie and Brown, 1994). Because the *myo2–66* allele encodes a point mutation in a region of the motor domain predicted to interact with actin, this suggests that some motor function may be required for localization (Lillie and Brown, 1994). Interestingly, in cells treated with an actin-depolymerizing drug, Latrunculin A, polarized Myo2p staining was observed (Ayscough *et al.*, 1997). Although fewer cells contained polarized Myo2p staining compared with wild-type cells, these data suggest that some aspect of Myo2p localization may be actin independent. In addition, a kinesin-related protein, Smy1p, originally identified by its ability to suppress the *myo2–66* phenotype, can partially restore Myo2p localization in *myo2–66* (Lillie and Brown, 1992, 1994). However, the role of Smy1p in Myo2p localization remains unclear (Lillie and Brown, 1998).

Few studies to date have investigated the role of the tail domain of a class V myosin in localization (Catlett and Weisman, 1998; Wu *et al.*, 1998). Furthermore, although the subcellular fractionation of class V myosins has been extensively studied in other systems, little is known about the subcellular fractionation of Myo2p. In this work, we use *S. cerevisiae* as a model system to study targeting of class V myosins. We have overexpressed the carboxyl-terminal-tail domain of Myo2p to investigate the role of the tail in targeting and function. Overexpression of the tail of Myo2p causes a dominant–negative phenotype. We find that the carboxyl-terminal tail of Myo2p is sufficient for localization to sites of polarized cell growth. Overexpression of the tail of Myo2p causes mislocalization of the endogenous Myo2p, suggesting that some critical and limiting localization determinant for Myo2p exists in the cell. We have also investigated the subcellular fractionation of Myo2p and find that Myo2p is associated with a 100,000 $\times$ *g* pellet.

Table 1. Strains used in this study

Strain	Genotype
NY59	Mat a *ura3-52 his4-619 sec9-4*
NY405	Mat a *ura3-52 sec4-8*
NY506	Mat α *ura3-52 his4-116 sec3-2*
NY604	Mat α *ura3-52 leu2-3,112*
NY1006	Mat a *ura3-52 leu2-3,112 myo2-66*
NY1443[a]	Mat α *ura3 leu2 trp1 his4 cdc42-1*
RPY1	Mat α *ura3-52 leu2-3,112*:: *(LEU2, GAL-MYO2 tail)*
RPY2	Mat α *ura3-52 leu2-3,112*:: *(LEU2, GAL)*
K5209[b]	Mat a *ade2, trp1, leu2, his3, ura3, can1, ho, MYO4*::*URA3*
YJC 1454[c]	Mat a/Mat α *MYO2-GFP-HIS3/MYO2-GFP-HIS3, leu2/leu2, ura3/ura3, his3-Δ200/his3-Δ200*

[a] Gift from A. Bender, Indiana University (Bloomington, IN).

[b] Gift from R. Singer, Albert Einstein University (New York, NY).

[c] Gift from J. Cooper, Washington University School of Medicine (St. Louis, MO).

MATERIALS AND METHODS

Yeast Strains and Media

The yeast strains used in this study are shown in Table 1. Yeast were grown in YP medium (1% Bacto yeast extract, 2% Bacto, peptone; Difco, Detroit, MI) containing either 2% dextrose, 2% glucose, 2% galactose, or 3% glycerol at 25°C. To induce expression from the *GAL1* promoter, log-phase cells grown in YP-dextrose were pelleted and resuspended in YP-glycerol, grown overnight, pelleted again, and resuspended in YP-galactose for varying periods of time.

Construction of MYO2DN

To epitope tag *MYO2*, site-directed mutagenesis was used to insert the 12CA5 hemagglutinin (HA) epitope at a unique *Bgl*II site (base pair [bp] 3388) in *MYO2* (pN444). The tagged copy of *MYO2* was functional as the sole copy of *MYO2* in the cell (Govindan, 1995). The *MYO2DN* construct was generated by PCR amplification from pN444 of 1464 bp (encoding amino acids 1087–1574) of the 3′-end of Myo2 plus 350 bp of 3′-untranslated region. The 5′-oligonucleotide contained a *Bam*HI site and the start codon ATG: 5′-GC**GGATC-C**ATGACCGTTACTACTAGTGTAC-3′. The 3′-oligonucleotide contained a *Xho*I site: 5′-GGC**CTCGAG**CATTATCATACTATTGAC-3′. The PCR product was ligated into pNB527 (a LEU, integrating yeast plasmid that contained the *GAL1* promoter) at *Bam*HI and *Xho*I. The resulting plasmid was sequenced. This plasmid was then linearized with *Cla*I (a unique restriction site within the *LEU2* gene) and transformed into the yeast strain NY604, creating *MYO2DN* (RPY1). To serve as a wild-type control, NY604 was also transformed with pNB527 containing no insert, creating strain RPY2.

Production of Myo2p Motor and Tail-Domain Antibodies

To prepare the Myo2p tail-domain antibody, a GST–Myo2p tail fusion protein was created by subcloning a 1.6-kilobase (kb) *Dra*I–*Hin*cII (encoding amino acids 1139–1562) fragment from the tail-encoding region of *MYO2* into pGEX-5X-1 (Pharmacia Biotech, Uppsala, Sweden). The fusion protein was induced and purified as described by the manufacturer (Pharmacia Biotech). To create a fusion protein for affinity purification, 1.47 kb (encoding amino acids 1087–1574) of the carboxyl-terminal tail-encoding region of *MYO2* were amplified by PCR using the following primers: 5′-primer, 5′-CG**GGATCC**ACCGTTACTACTAGTGTAC-3′; and 3′-primer, 5′-AA**CTGCAG**GTGGCCGTCTTGAACGAC-3′ and cloned into pMAL-p2 (New England Biolabs, Beverly, MA). The fusion protein was induced and purified as described by the manufacturer (New England Biolabs). The maltose binding protein (MBP)–Myo2p fusion protein was covalently linked to a CnBr-activated Sepharose column as described by the manufacturer (Pharmacia Biotech).

To prepare the Myo2p-motor-domain antibody, a MBP–Myo2p fusion protein was created by subcloning a 135-bp fragment of the Myo2p motor domain (encoding amino acids 596–640) that was generated by PCR using the following oligonucleotides: 5′-primer, 5′-CG**GAATTC**TCTACCA-ACGAGACACTAA-3′; and 3′-primer, 5′-AA**CTGCAG**TCATTTCCTGTTAACCGTTCTT-3′ into pMAL-p2 (New England Biolabs). This region of the Myo2p motor domain is one of the few regions of the motor domain that is not highly conserved with Myo4p. To create a fusion protein for affinity purification, the same region was amplified by PCR using the following primers: 5′-primer, 5′-CG**GAATTC**TCTACCAACGAGACACTAA-3′; and 3′-primer, 5′-CCG**CTCGAG**TCATTTCCTGTTAACCGT-TCTT-3′ and subcloned into pGEX-5X-1 (Pharmacia Biotech). The GST–Myo2p motor domain fusion protein was covalently linked to a CnBr-activated Sepharose column as described by the manufacturer (Pharmacia Biotech).

Quantitation of Expression Levels of Myo2p and HA-tagged Tail

Yeast lysates were prepared using 10 ml of cells at an A_{600} of 0.5. The cells were spun down and washed in 10 mM sodium azide, 10 mM Tris, pH 7.5. The cells were then resuspended in ice-cold 10 mM sodium azide, 10 mM Tris, pH 7.5, 1 mM Pefabloc (Boehringer Mannheim, Indianapolis, IN), 10 mM Pepstatin A (Sigma Chemical, St. Louis, MO) and lysed by vortexing for 3 min at 4°C using 0.5-mm glass beads. The lysate was spun at 2,000 × *g* for 2 min to remove glass beads and unbroken cells, and the protein concentration of the resulting supernatant was calculated by BCA (Pierce Chemical, Rockford, IL) assay. To determine expression levels of the HA-tagged tail and endogenous Myo2p in galactose time course experiments, equal protein concentrations of each sample were separated by SDS-PAGE and immunoblotted with affinity-purified anti-Myo2p head antibody (0.6 μg/ml) or an antibody to the HA epitope tag (Clone 12CA5, 1:2000). To determine the relative amounts of Myo2p tail and endogenous Myo2p, lysates were separated by SDS-PAGE along with known amounts of GST–Myo2p tail fusion protein. Such gels were immunoblotted with anti-Myo2p tail (0.15 μg/ml) or anti-HA antibody. The immunoreactive bands were visualized by ECL, and the films were scanned and analyzed using Metamorph (Universal Imaging, West Chester, PA).

Thin-Section Electron Microscopy (EM)

MYO2DN and wild-type cells were grown to early-log phase in YP-glycerol–containing medium. The cells were then spun down and grown for 1, 3, or 6 h in YP-galactose–containing medium. The cells were then fixed, stained, and sectioned as previously described (Salminen and Novick, 1987).

Immunofluorescence Microscopy

MYO2DN and wild-type cells were grown as described above. Cells were fixed in 2% glucose, 20 mM EGTA, 3.7% formaldehyde in PBS (Finger and Novick, 1997). The fixed cells were then processed as previously described (Roth *et al.*, 1998). Primary antibodies were incubated for 1 h at room temperature or overnight at 4°C using the following dilutions in PBS, 1 mg/ml BSA, 1% normal goat serum: monoclonal anti-Sec4p, 1:10 (clone C1.2.3); polyclonal anti-Myo2p tail, 0.4 μg/ml; polyclonal anti-Myo2p head, 4.8 μg/ml; monoclonal anti-actin 1:500 (clone C4, Sigma); monoclonal anti-HA (clone 12CA5), 1:500. Secondary antibodies were diluted in the same block-

ing reagent and used at the following dilutions: CY3-conjugated goat anti-rabbit IgG (Jackson Laboratories, West Grove, PA), 1:300; CY3-conjugated goat anti-mouse IgG (Jackson Laboratories), 1:300.

Cells were observed using a Nikon (Garden City, NY) Diaphot 300 equipped with a 100×, 1.4 NA objective. Images were captured using a cooled, charge-coupled-device (CCD) camera. The camera recordings were controlled by Metamorph (Universal Imaging). Quantitation was performed by randomly selecting fields and scoring all cells in that field for polarity of Myo2p or Sec4p.

Cell Fractionation

Log-phase *MYO2DN* or wild-type cells (100 ml) were grown overnight in glycerol and then shifted to galactose for 1, 3, or 6 h. The cells were spun down, washed once with water, and lysed in either 1 mM EGTA, 50 mM Tris, pH 7.5, 40 mM KCl, 0.1 mM DTT, 2 mM Pefabloc-sc, 1 mM benzamidine, 10 mM leupeptin, chymostatin, and pepstatin or 300 mM sucrose, 20 mM HEPES, pH 7.2, 1 mM EGTA, 1 mM $MgCl_2$ plus protease inhibitors. The fractionation pattern of Myo2p remained the same using either lysis buffer. In initial experiments, cells were lysed by spheroplasting. However, we found that under these conditions we did not observe polarized Myo2p localization, as assayed by immunofluorescence. Due to this observation, we used a mechanical lysis protocol for all experiments presented in this work. Cells were lysed with 0.5 mM zirconium/silica beads (Bio Spec Products, Bartlesville, OK) using a Mini-BeadBeater-8 (Bio Spec Products) for 2 × 45 s at 4°C. The resulting lysate was spun at 2,500 × *g* for 10 min to pellet unbroken cells and beads. The resulting supernatant was spun at 30,000 × *g* for 30 min. The 30,000 × *g* supernatant was then spun at 100,000 × *g* for 1 h. When testing the solubility of Myo2p, 1% Triton X-100, 0.6 M NaCl, or 5 mM Mg^{++}-ATP was added to the 30,000 × *g* supernatant, and this was spun at 100,000 × *g* for 1 h. Gel samples were made using volumetric stoichiometry, and equal volumes of each sample were then run on SDS-PAGE, transferred to polyvinylidene fluoride (PVDF), and immunoblotted using anti-Myo2p head (0.6 μg/ml), anti-HA (1:2000), or anti-Pma1p (0.5 μg/ml, a generous gift of C. Slayman, Yale University, New Haven, CT).

The temperature-sensitive strains, *sec4–8, sec9–4, sec3–2,* and *myo2–66*, were grown at the restrictive temperature (37°C) for 2 h before immediate lysis. The temperature-sensitive strain *cdc42–1* was grown at the restrictive temperature (37°C) for 3 h before immediate lysis.

Immunoprecipitations

MYO2DN and wild-type cells were grown to log phase in YP-glycerol–containing medium. The cells were then spun down and resuspended in YP-galactose–containing medium. After 1 h of growth in galactose-containing medium, the cells were harvested, washed, and resuspended in IP buffer (300 mM sucrose, 20 mM HEPES, pH 7.2, 1 mM EGTA, 1 mM $MgCl_2$, 0.1 mM DTT, 2 mM Pefabloc-sc, 1 mM benzamidine, 10 mM leupeptin, chymostatin, and pepstatin). The cells were lysed as described above for the cell fractionation. The lysate was spun at 2,000 × *g* for 10 min to remove unlysed cells and beads. The resulting supernatant was then spun at 100,000 × *g* for 1 h. The pellet fraction was resuspended in IP buffer to be equal in volume to the 100,000 × *g* supernatant. The supernatant and resuspended pellet were incubated with Protein A Sepharose CL-4B (Pharmacia Biotech) for 30 min as a preclear step. After the preclear beads were removed, 500 μl of anti-HA 12CA5 tissue culture supernatant were added per 1 ml of supernatant or reuspended pellet fraction. This mixture was incubated for 2 h at 4°C. Protein A Sepharose beads (3 μg) were then added to the lysate, and this mixture was incubated at 4°C for 1 h. The beads were then washed five times with 1 ml of IP buffer containing 150 mM KCl. The beads were boiled in sample buffer, and equal relative volumes of immunoprecipitates and the unbound fractions were separated by SDS-PAGE and transferred to PVDF. Immunoblots were performed using either polyclonal anti-HA antibody (Santa Cruz Biotechnology, Santa Cruz, CA) to test IP efficiency or anti-Myo2p head antibody (to test for tail association with the endogenous Myo2p).

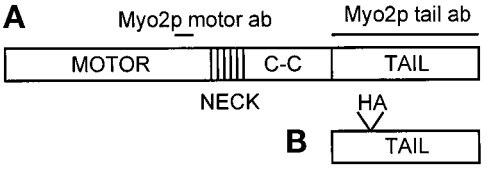

Figure 1. Schematic diagram of Myo2p, Myo2p tail construct, and anti-Myo2p antibodies. (A) The domain structure of the full-length Myo2p protein. Lines above the schematic indicate regions of Myo2p used to produce the motor- and tail-domain antibodies used in this study. The DNA encoding the tail domain of Myo2p (B), which did not include any of the region predicted to form α-helical coiled coil, was overexpressed behind the *GAL1* promoter to produce the yeast strain *MYO2DN*. Conventionally, the entire region after the neck domain is referred to as the "tail"; however, in this work we refer to the region after the coiled coil as the "tail".

RESULTS

Overexpression of the Tail Domain of Myo2p Produces a Dominant–Negative Phenotype

To gain information about the function of the carboxyl-terminal tail domain of Myo2p, we created a construct that was designed to overexpress this domain of Myo2p (Figure 1). The rationale behind this approach is that the tail domain of Myo2p may interact with certain molecules. Thus, overexpression of the tail domain could competitively inhibit the function of the endogenous Myo2p by binding to one of its partners. To create the Myo2p-tail-overexpression construct, the DNA encoding the carboxyl-terminal 487 amino acids of Myo2p was expressed behind the inducible *GAL1* promoter. The amino acids encoded by the tail construct do not contain amino acids in the tail of *MYO2* that are predicted to form an α-helical coiled coil. To differentiate the overexpressed tail from endogenous Myo2p, the tail was tagged with a single copy of the HA epitope. The full-length tagged copy of *MYO2* is functional as the sole copy of *MYO2* (Govindan *et al.*, 1995), suggesting that the presence of the HA tag does not interfere with tail function in the cell.

To analyze whether overexpression of the tail of Myo2p was deleterious, the growth of yeast transformed with the *GAL1*-tail construct or the *GAL1* vector alone was compared after a switch to galactose-containing medium for varying periods of time. Yeast transformed with the *GAL1*-tail construct grew slowly in liquid galactose-containing medium (conditions that induce expression from the *GAL1* promoter) in comparison with yeast cells transformed with the *GAL1* vector alone (Figure 2A).

We made two Myo2p-specific antibodies, an antibody directed to the motor domain (amino acids 596–

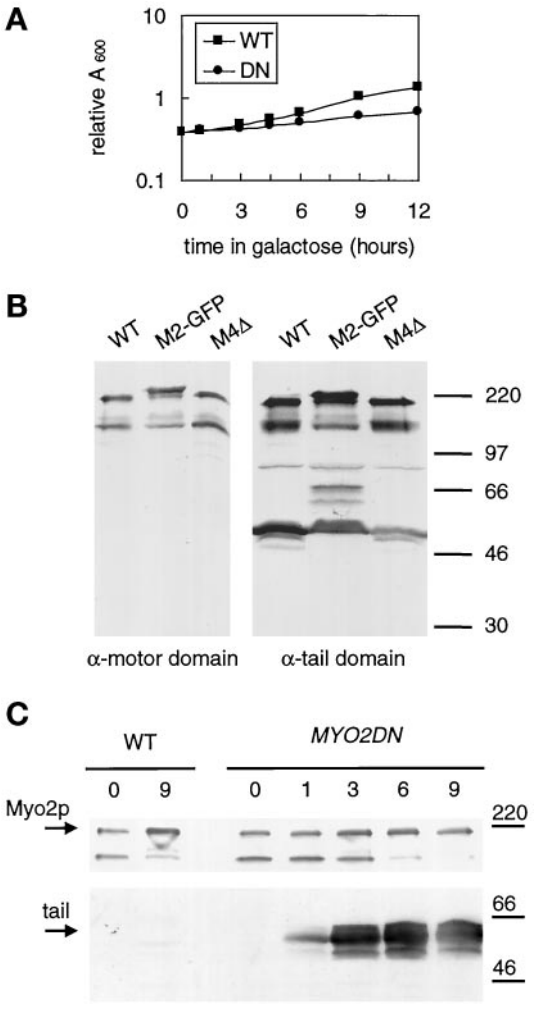

Figure 2. Overexpression of the tail of Myo2p causes a dominant–negative phenotype. *MYO2DN* (DN) and wild-type (WT) cells were grown in YP-glycerol and then shifted to YP-galactose for varying amounts of time. At each time point the A_{600} was measured (A), and protein samples were made (C). (A) The growth of cells transformed with the *GAL1* vector (WT) or *GAL1*–Myo2p tail (*MYO2DN)* was monitored by reading the A_{600} at 1, 3, 4.5, 6, and 9 h after a shift to galactose-containing medium. (B) Both motor- and tail-domain antibodies are specific for Myo2p. Wild-type (WT), Myo2-GFP (M2-GFP), and Myo4 knock-out (M4Δ) cells were lysed, and gel samples from each strain were separated by SDS-PAGE and immunoblotted using affinity- purified anti-Myo2p motor domain antibody or anti-Myo2p tail antibody. The immunoblot using the Myo2p-tail antibody was overexposed so that the ~70 kDa GFP-specific breakdown product could be visualized. Molecular weight markers are indicated on the right-hand side of the immunoblots. (C) Immunoblots using anti-Myo2p head or an anti-HA antibody reveal expression levels of the endogenous Myo2p and tail, respectively, at each time point. Equal amounts of total protein were loaded in each lane. Relative amounts of overexpressed tail were determined using scanning densitometry. Molecular weight markers are indicated on the right-hand side of the immunoblots.

640) and an antibody directed to the tail domain (amino acids 1087–1574, Figure 1). Both antibodies recognized a ~180-kDa band on Western blots of total cell lysates (Figure 2B). Both antibodies also recognized an additional band of ~130 kDa (Figure 2B). This band most likely represents a large motor domain fragment, which contains a small amount of the tail domain, as both the head and tail antibodies recognize this degradation product (Figure 2B). The tail antibody recognizes an additional ~50-kDa breakdown product, which is not recognized by the motor-domain antibody. Thus, it seems that there is a site near the beginning of the globular tail that is easily proteolized. To confirm the specificity of the antibodies, both a *MYO4* deletion strain and *MYO2*-GFP cells were immunoblotted with each antibody. No bands were absent in the *MYO4* deletion strain, confirming that neither antibody reacts with Myo4p. Both antibodies recognized a slightly larger protein in the *MYO2*-GFP strain, confirming that the 180-kDa band is Myo2p. An additional ~70-kDa breakdown product is seen in the *MYO2*-GFP strain. This breakdown product most likely represents a tail fragment as Myo2p was GFP tagged at its carboxyl terminus.

To determine expression levels of the tail and endogenous Myo2p, quantitative densitometry of immunoblots was performed using known amounts of bacterially expressed Myo2p-tail-fusion protein as standards. In wild-type cells, Myo2p represents ~0.001% of the total cell protein. The expression level of Myo2p did not change in cells overexpressing the tail (Figure 2C). In cells overexpressing the tail, expression levels of the HA-tagged tail increased with time on galactose (Figure 2C). After 1 h of growth on galactose, tail expression levels were 10 times that of the endogenous Myo2p. By 3 h, tail levels had reached a maximum expression level of 50 times that of the endogenous Myo2p. Thus, expression levels of the tail increase rapidly upon a switch to galactose medium, suggesting that high levels of expression of Myo2p are toxic to the cell. As overexpression of the tail of Myo2p caused a dominant-negative phenotype, we have named the strain that overproduces the tail of Myo2p *MYO2* dominant-negative (*MYO2DN*).

The Tail Domain of Myo2p Is Sufficient for Localization

To determine whether the tail domain of Myo2p is sufficient for localization, we used the anti-HA antibody to examine the localization of the overexpressed tail in *MYO2DN* cells by indirect immunofluorescence microscopy. In wild-type cells, Myo2p localizes to sites of polarized growth such as the bud tip of small budded cells (Lillie and Brown, 1994). After a short (1 h) shift to galactose-containing medium the overexpressed tail localized to the bud of dividing cells (Figure 3, A–F). Tail localization was observed in 23 ± 7% of cells grown in galactose for 1 h. Thus, the carboxyl-terminal-tail domain of Myo2p is sufficient for local-

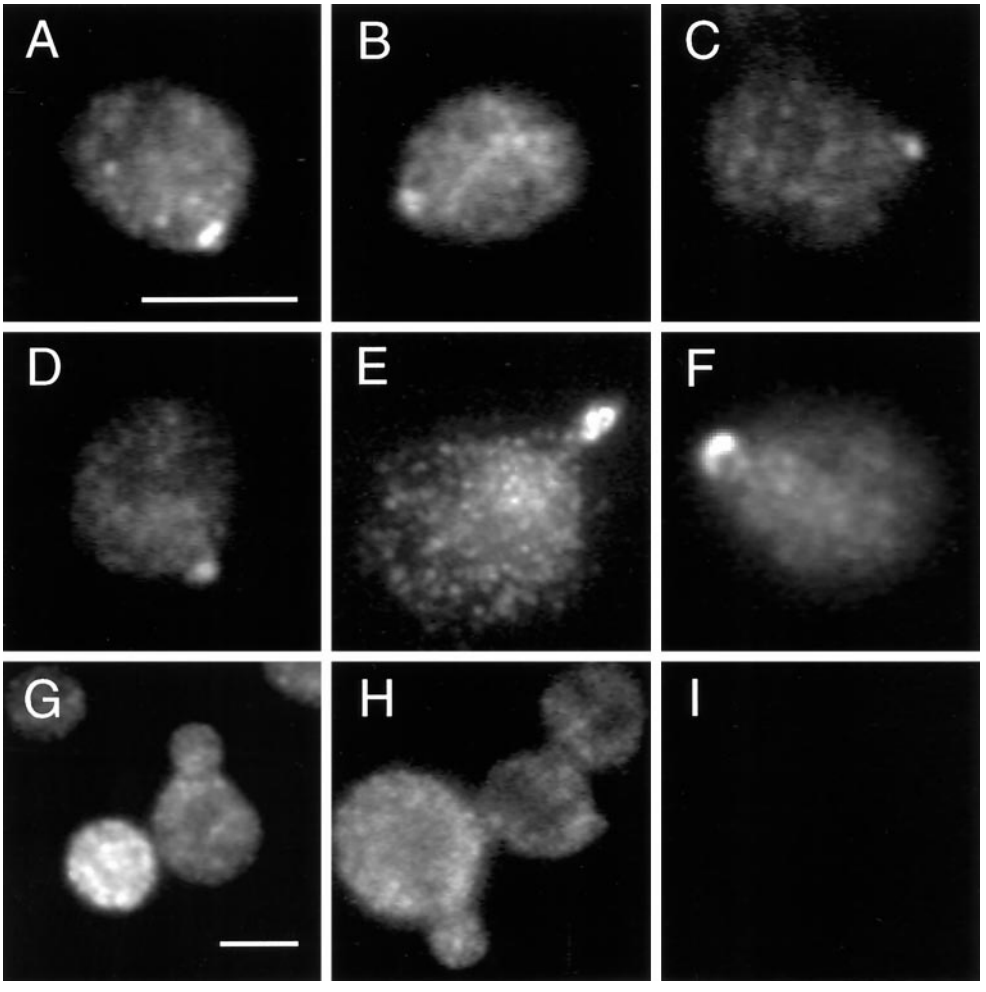

Figure 3. The tail domain of Myo2p is sufficient for localization. *MYO2DN* cells were grown in galactose for 0 (I), 1 (A–F), or 3 h (G and H), fixed, and stained using anti-HA antibody. The tail localized to the bud tip after a 1-h shift to galactose; 23 ± 7% of the cells demonstrated polarized Myo2p staining. After 3 h of growth on galactose, polarized staining was no longer observed. Scale bar, 5 μm.

ization. After short shifts to galactose, the intensity of staining with the anti-HA antibody was variable from cell to cell, suggesting that expression levels of the tail were variable. Dimly stained cells rarely showed tail localization, suggesting that in these cells expression levels were too low to detect tail localization. Polarized tail staining was observed in brightly stained cells.

After 3 h of growth on galactose medium, the tail was no longer polarized (Figure 3, G and H). Expression levels of the tail increased ~40-fold between the 1- and 3-h time points (Figure 2C), most likely resulting in the mislocalization observed. Specifically, high levels of tail expression could cause saturation of any polarized tail-binding site. Alternatively, such a polarized binding site may no longer be polarized after 3 h of growth in galactose, as *MYO2DN* cells are depolarized by this time point (see below).

MYO2DN Cells Stop Budding and Accumulate Vesicles

To determine whether *MYO2DN* cells had a *myo2–66*-like phenotype, we assayed *MYO2DN* for a number of phenotypes that have been reported for the temperature-sensitive allele of *myo2*, *myo2–66*.

To examine whether *MYO2DN* cells stop budding, cells were grown in glycerol-containing medium and shifted to galactose-containing medium for various amounts of time. At each time point, the number of unbudded, small-budded, and large-budded cells was determined (Table 2). Wild-type cells grown in glycerol spend a greater proportion of the cell cycle in G_1 (Jagadish and Carter, 1977). Consistent with this observation, we found that 80% of wild-type or *MYO2DN* cells were unbudded after overnight growth in glycerol. The glycerol shift was used to

Table 2. Wild-type (WT) and *MYO2DN* (DN) cells were grown in glycerol overnight and then switched to galactose-containing medium for varying periods of time

Hours in galactose	Genotype	Unbudded (%)	Small budded (%)	Large budded (%)
0	WT	80	10	11
	DN	80	8	13
1	WT	60	23	18
	DN	69	16	15
3	WT	26	27	42
	DN	69	16	15
6	WT	33	25	43
	DN	75	9	16
9	WT	37	17	47
	DN	76	7	17

At each time point the number of unbudded, small-budded, and large-budded cells was determined (n = 400 for each genotype at each time point).

allow rapid induction of the galactose promoter. After 1 h of growth in galactose, both wild-type and *MYO2DN* cells began to resume budding. After 3 h of growth in galactose 67% of the wild-type cells were budded, whereas only 31% of the *MYO2DN* cells were budded. Thus, overexpression of the tail of Myo2p results in decreased budding efficiency.

Thin-section EM of *MYO2DN* yeast cells revealed the accumulation of cytoplasmic vesicles after 1, 3, and 6 h of growth in galactose-containing medium (Figure 4, C–E). The number of vesicles per cell increased with time in galactose-containing medium. Aberrant Golgi-like structures (referred to as Berkeley bodies; Novick and Botstein, 1985) and ordered arrays of unknown composition were observed only at the 6-h time point (Figure 4E). These structures were not observed in wild-type cells grown in galactose for 6 h (Figure 4A). The ordered arrays may represent actin bars because the timing of their appearance correlates with the appearance of actin bars as assayed by indirect-immunofluorescence microscopy (see below). Actin bars have been observed by immunofluorescence in a number of mutants that affect the actin cytoskeleton, including *myo2–66*; however, their appearance at the EM level has not previously been described (Novick and Botstein, 1985; Liu and Bretscher, 1989; Novick *et al.*, 1989; Haarer *et al.*, 1990). Filament bundles hypothesized to be actin bundles have been previously observed in yeast cells (Adams and Pringle, 1984). However, these bundles appear to be morphologically distinct from the ordered arrays observed in *MYO2DN*.

The accumulation of cytoplasmic vesicles in *MYO2DN* cells appears to be the primary phenotype observable by EM, whereas the appearance of Berkeley bodies and the putative actin bars is most likely an indirect effect of loss of *myo2* function, as these phenotypes are only observed at a late time point. *myo2–66* cells also stop budding and accumulate Berkeley bodies and cytoplasmic vesicles. Given the similarity between the *myo2–66* phenotype and the *MYO2DN* phenotype, we can conclude that overexpression of the tail of Myo2p is toxic because it interferes with the function of the endogenous Myo2p.

Actin is Mislocalized in MYO2DN

In wild-type yeast cells, actin is found in both patches and cables. During budding, actin patches are found primarily in the daughter cell and actin cables can be seen running between mother and daughter cells (Adams and Pringle, 1984; Kilmartin and Adams, 1984; Novick and Botstein, 1985). In *myo2*-66 cells, actin patches are depolarized and abnormal actin bars are detected (Johnston *et al.*, 1991). Effects of Myo2p tail overexpression on the actin cytoskeleton were examined using the monoclonal anti-actin antibody, C4, in glycerol-grown cells and after shifts to galactose for varying periods of time. In glycerol, both wild-type and *MYO2DN* cells had a largely depolarized actin cytoskeleton, most likely due to the fact that 80% of the cells grown in glycerol are unbudded (Figure 5, A and B). Alternatively, the yeast actin cytoskeleton is known to be sensitive to a variety of stresses, one of which could be glycerol growth (Chowdhury *et al.*, 1992). After a 1-h shift to galactose, actin patches were present primarily in the daughter cells of budding cells, and actin filaments could be observed in both wild-type and *MYO2DN* cells (Figure 5, C and D). After 3 h of growth in galactose, actin localization was qualitatively normal in *MYO2DN* cells, although fewer cells were budded and 4% (n = 122) of the cells contained actin bars (our unpublished results). *MYO2DN* cells grown in galactose for 6 h had very aberrant actin localization: 85% (n = 107) of the cells contained either actin bars or abnormally large actin patches (Figure 5F). Thus, as has been observed in *myo2–66* cells, overexpression of the tail domain of Myo2p disrupts the localization of the actin cytoskeleton.

MYO2DN Cells Are Depolarized

To determine when and if *MYO2DN* cells depolarize, the localization of Sec4p was examined in *MYO2DN* cells. Sec4p is a rab protein that functions at the post-Golgi stage of the secretory pathway in yeast (Novick and Zerial, 1997). Sec4p can be considered a marker for the polarized state of the yeast- secretory pathway

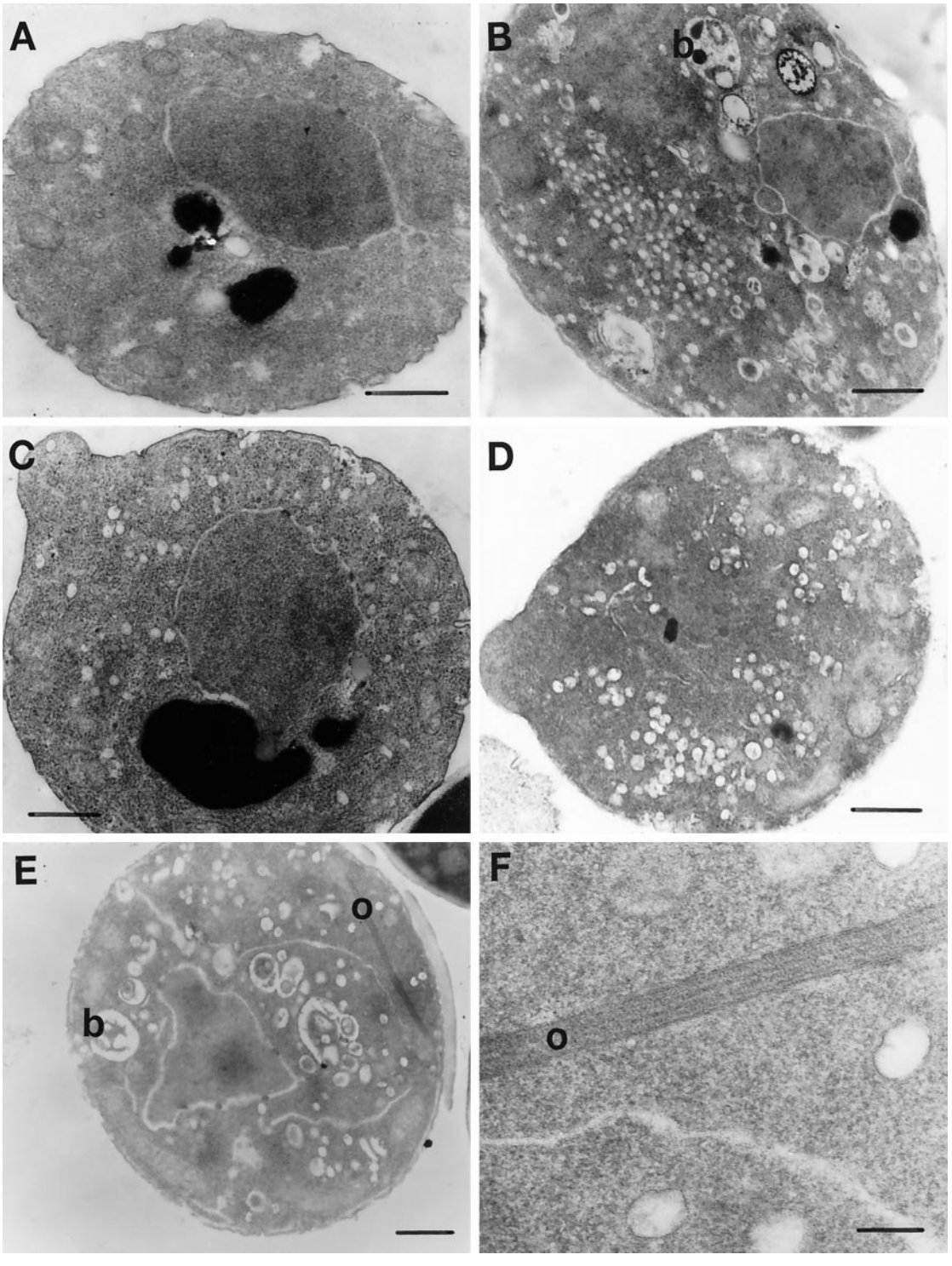

Figure 4. Thin-section EM of *MYO2DN.* Wild-type (WT) cells were grown in YP-galactose for 6 h (A). *myo2–66* cells were grown in YP-dextrose at 37°C for 20 min (B). *MYO2DN* cells were grown in galactose for 1 (C), 3 (D), or 6 h (E and F). Berkeley bodies (b) were observed in *myo2–66* after 20 min at the restrictive temperature and *MYO2DN* cells at the 6-h time point. Ordered arrays (o), which may represent actin bars, were observed in *MYO2DN* at the 6-h time point (E and F). Scale bar, 500 nm (A–E); 100 nm (F).

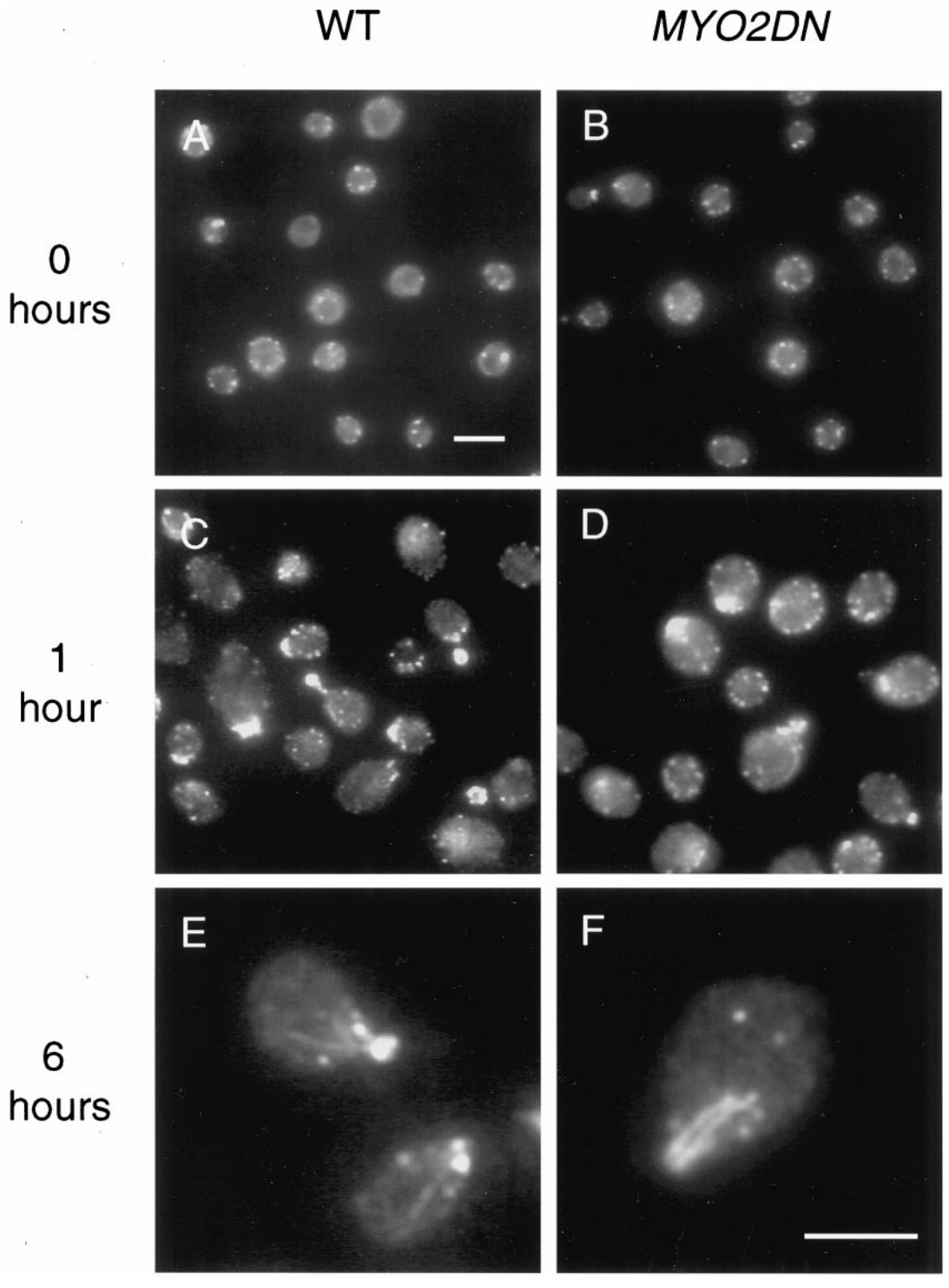

Figure 5. Actin localization in *MYO2DN*. Wild-type (WT) and *MYO2DN* cells were grown in glycerol (A and B) and shifted to galactose for 1 (C and D) or 6 h (E and F), fixed, and stained with anti-actin antibody. After a 1-h shift to galactose, actin patches were polarized to the buds of dividing cells, and actin filaments could be detected. After 6 h of growth in galactose, 85% (n = 107) of the cells observed had abnormal actin bars or large patches. Scale bar, 5 μm (A–D); 5 μm (E and F).

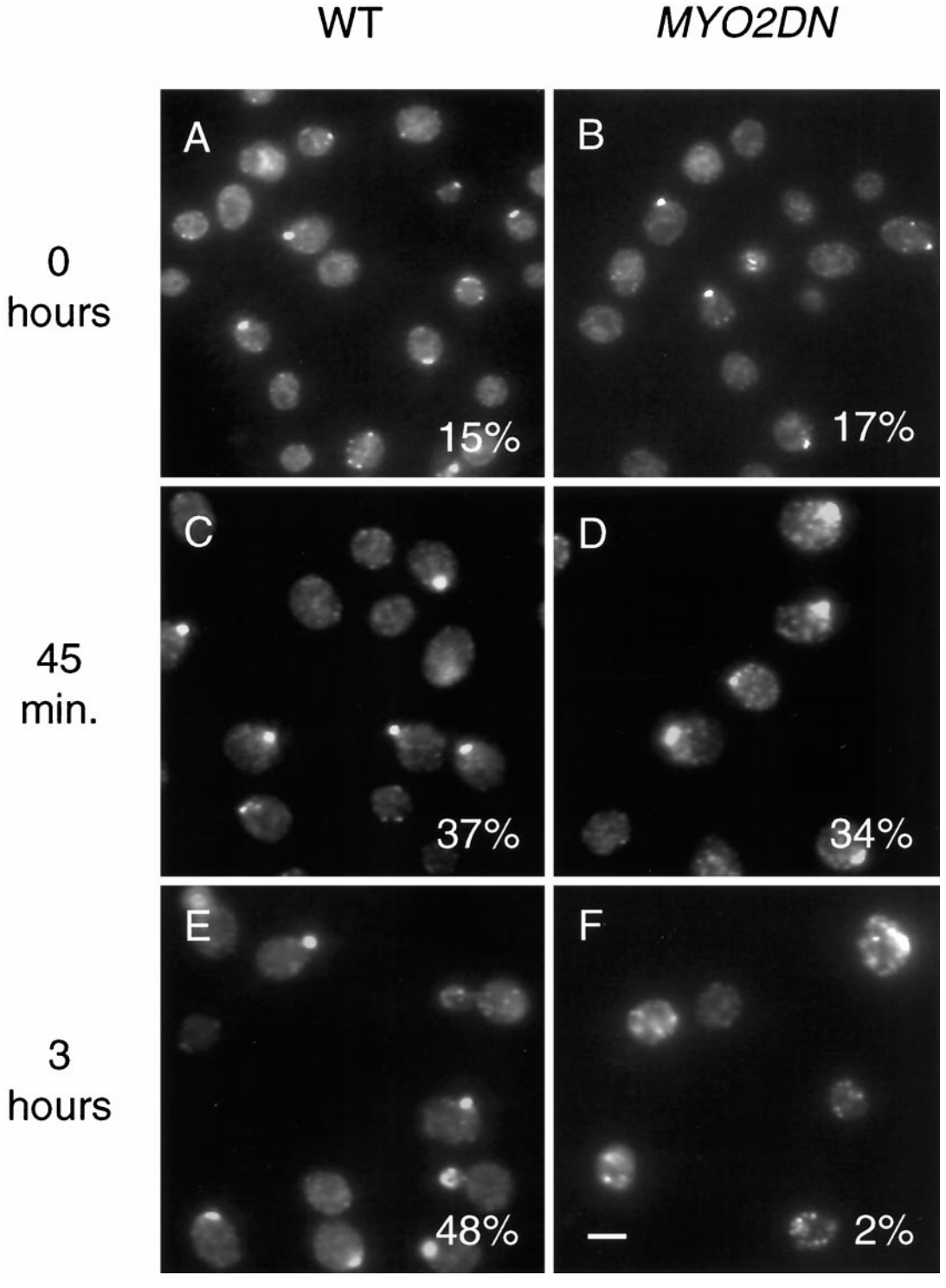

Figure 6. Sec4p localization in *MYO2DN*. Wild-type (WT) and *MYO2DN* cells were grown in glycerol (A and B) and shifted to galactose for 45 min (C and D) or 3 h (E and F), fixed, and stained using anti-Sec4p antibody. Sec4p staining was polarized in wild-type cells or *MYO2DN* cells grown in glycerol (n = 200) or galactose for 45 min (n =400). After 3 h in galactose only 2% (n =409) of *MYO2DN* cells observed had polarized Sec4p staining. Scale bar, 5 μm.

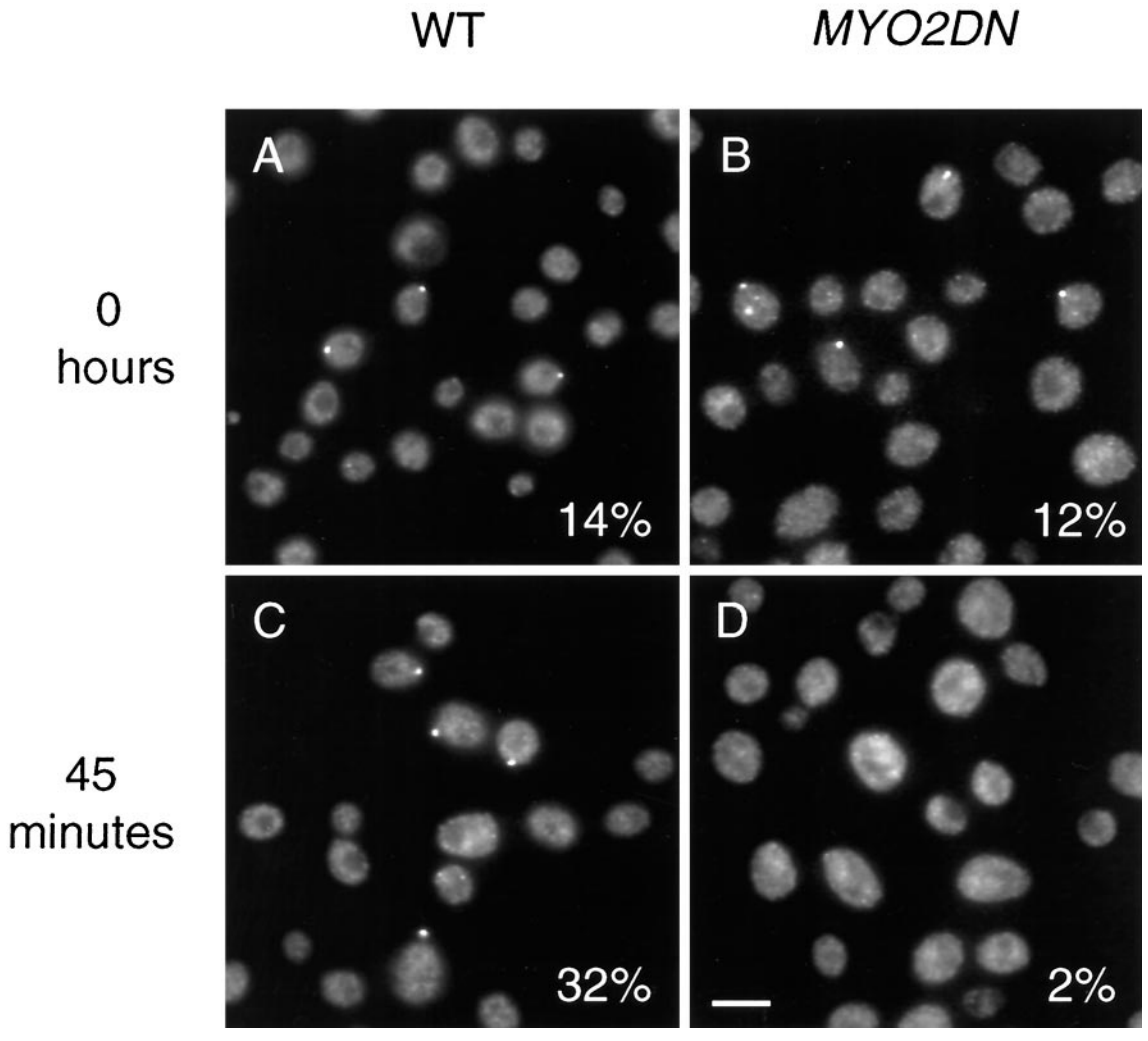

Figure 7. Overexpression of the tail of Myo2p causes the endogenous Myo2p to delocalize. Wild-type (WT) and *MYO2DN* cells were grown in glycerol (A and B) and shifted to galactose for 45 min (C and D), fixed, and stained with anti-Myo2p head antibody. Myo2p was localized to the bud in wild-type and *MYO2DN* cells grown in glycerol (n = 200) and in wild-type cells grown in galactose for 45 min (n = 420), but was delocalized in *MYO2DN* cells grown in galactose for 45 min (n = 402). Scale bar, 5 μm.

because its localization correlates with regions of polarized yeast cell growth, such as the bud tip of small budded cells (Novick and Brennwald, 1993). In glycerol-grown cells ~16% (n = 400) of wild-type or *MYO2DN* cells had polarized Sec4p staining (Figure 6, A and B). After 45 min of growth in galactose, Sec4p was polarized in ~35% (n = 200) of either wild-type or *MYO2DN* cells (Figure 6, C and D). However, the staining of Sec4p in *MYO2DN* cells appeared to be slightly more diffuse compared with wild-type cells (Figure 6D). After 3 h of growth on galactose, Sec4p staining was no longer polarized in *MYO2DN* cells (Figure 6F). These results show that *MYO2DN* cells are depolarized after 3 h of growth on galactose-containing medium.

Endogenous Myo2p Is Rapidly Mislocalized in MYO2DN

To investigate the mechanism by which overexpression of the tail of Myo2p caused a dominant–negative phenotype, we used an antibody directed against the motor domain of Myo2p to specifically localize the endogenous Myo2p in *MYO2DN* cells. Myo2p was polarized in ~13% (n = 200) of either wild-type or *MYO2DN* cells (Figure 7, A and B). This result was similar to that observed for Sec4p in glycerol-grown cells (Figure 6, A and B). In wild-type cells grown in galactose for 45 min, 32% (n = 420) of the cells had polarized Myo2p staining (Figure 7C). In contrast, in *MYO2DN* cells grown in galactose for 45 min, only 2%

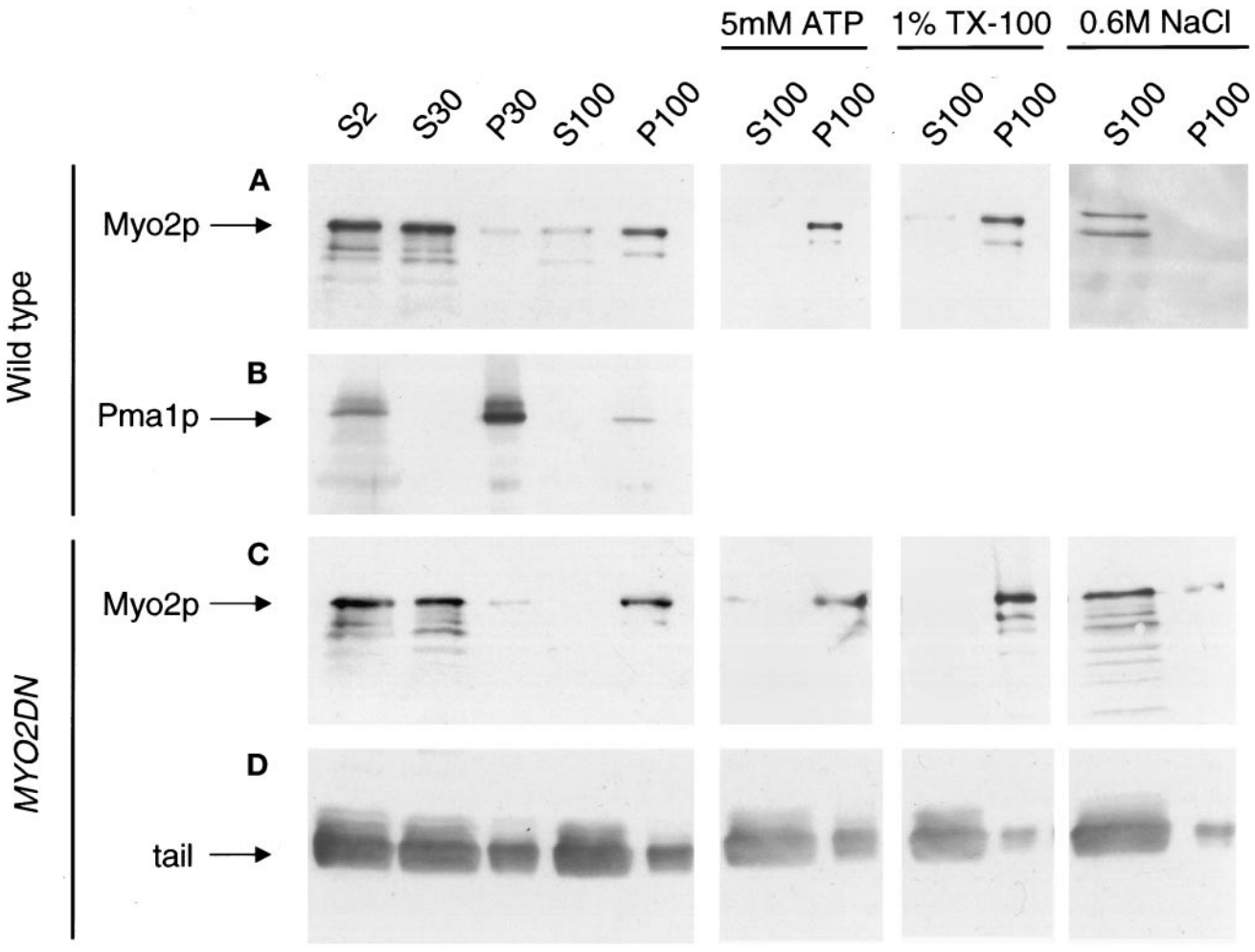

Figure 8. Subcellular fractionation of wild-type and *MYO2DN* cells. Wild-type (A and B) and *MYO2DN* (C and D) cells were grown in galactose for 3 h. Cells were harvested, and the resulting lysate was spun at 2,000 × *g* to generate supernatant 2 (S2). S2 was spun at 30,000 × *g*, resulting in S30 and pellet 30 (P30). S30 was spun at 100,000 × *g* to generate S100 and P100. To investigate the solubility of Myo2p, 5 mM Mg-ATP, 1% Triton X-100, or 0.6 M NaCl was added to S30, which was then spun at 100,000 × *g*, yielding S100 and P100. Gel samples were prepared using volumetric stoichiometry, and equal volumes of each sample were loaded per lane, separated by SDS-PAGE, and transferred to PVDF. The blots were then probed with anti-Myo2p head antibody (A and C), anti-Pma1p (B), or anti-HA (D). The majority of the Myo2p was found in the 100,000 × *g* pellet. The Myo2p in this pellet was not released by tail overexpression, Mg–ATP, or Triton X-100, but was solubilized by 0.6 M NaCl.

(n = 402) of the cells had polarized Myo2p staining (Figure 7D). Endogenous Myo2p remained depolarized in *MYO2DN* cells grown in galactose for longer periods of time (our unpublished results). These results suggest that the overexpressed tail is toxic because it competes with the endogenous Myo2p for some factor that is critical for localization.

Myo2p Is Found in a 100,000 × g Pellet

Another means to investigate the effects of tail overexpression is to examine the subcellular fractionation of the endogenous Myo2p. Because the subcellular fractionation of Myo2p has not been investigated previously, we first characterized Myo2p in wild-type cells using differential centrifugation. Nearly all of the Myo2p in the cell can be found in a 100,000 × *g* pellet after homogenization by mechanical lysis (Figure 8A). Negative-stain EM analysis revealed that this pellet fraction consisted of small vesicles (50–100 nm) and 30-nm particles that may represent ribosome subunits (our unpublished results). A marker for the plasma membrane in yeast, Pma1p, was found primarily in the 30,000 × *g* pellet, which contained very little detectable Myo2p (Figure 8B). The Myo2p in the

100,000 × *g* pellet was not extracted by either 5 mM Mg^{++}–ATP or 1% Triton X-100, suggesting that Myo2p pellet association is not actin dependent and is not due to a direct membrane interaction (Figure 8A). The addition of 0.6 M NaCl was sufficient to solubilize all of the Myo2p in the 100,000 × *g* pellet (Figure 8A).

The fractionation pattern of Myo2p was also examined in a number of mutant yeast strains. The *myo2–66* allele of *MYO2* contains a point mutation in a region of the motor domain predicted to interact with actin (Lillie and Brown, 1994). Because the fractionation pattern of Myo2p did not change in *myo2–66* cells grown at the restrictive temperature, we can conclude that this point mutation does not affect Myo2p pellet association (our unpublished results).

As *MYO2* genetically interacts with many genes that function in the post-Golgi secretory pathway, the fractionation of Myo2p was examined in *sec4, sec3,* and *sec9* mutants (Govindan *et al.*, 1995). Sec4p is a member of the rab family of guanosine triphosphatases (Novick and Zerial, 1997). Sec3p is one of the first proteins to mark where polarized secretion will occur (Finger *et al.*, 1998). Sec9p is a t-SNARE that resides on the plasma membrane (Brennwald *et al.*, 1994). No changes in the fractionation pattern of Myo2p were observed in *sec4–8, sec3–2,* or *sec9–4* cells grown at the restrictive temperature (our unpublished results). *sec4, sec9*, and *sec3* mutants all accumulate secretory vesicles when grown at the restrictive temperature. In these mutants, vesicles are unable to dock or fuse with the plasma membrane. Thus, blocking secretory vesicle docking and fusion does not affect the ability of Myo2p to associate with the 100,000 × *g* pellet.

Finally, as pellet association of Myo2p may depend on cell polarity, the subcellular fractionation of Myo2p was examined in *cdc42–1*, a mutant that disrupts cell polarity (Chant, 1996). In *cdc42–1* cells grown at the restrictive temperature, Myo2p fractionation remained unchanged (our unpublished results).

Interestingly, if cells were lysed by hypotonic lysis after cell wall removal, nearly all of the Myo2p was soluble, yet unproteolyzed, indicating that cell wall integrity may be important for Myo2p pellet association (our unpublished results). Indirect immunofluorescence microscopy of Myo2p in these spheroplasted cells revealed that cell wall removal also caused delocalization of Myo2p from the bud tip (our unpublished results).

Overexpression of the Tail Does Not Release Endogenous Myo2p from the 100,000 × g Pellet

To further define the mechanism by which overexpression of the tail of Myo2p caused a dominant–negative phenotype, the subcellular fractionation of the endogenous Myo2p was examined in *MYO2DN*. In *MYO2DN* cells grown in galactose for 3 h, the endogenous Myo2p remained associated with the 100,000 × *g* pellet (Figure 8C). The endogenous Myo2p also remained associated with the 100,000 × *g* pellet in *MYO2DN* cells that were grown in galactose for 1 or 6 h (our unpublished results). In *MYO2DN* cells, the endogenous Myo2p remained in the pellet in the presence of 1% Triton X-100 and 5 mM Mg^{++}–ATP, but was solubilized by 0.6 M NaCl, as was the case in wild-type cells (Figure 8C). As assessed using the anti-HA antibody, after 3 h of growth in galactose the overexpressed tail was largely soluble, although some protein was detected in both the 30,000 × *g* and 100,000 × *g* pellets (Figure 8D). Thus, whereas overexpression of the tail of Myo2p causes mislocalization from sites of polarized cell growth, it does not release Myo2p from a sedimentable fraction.

Endogenous Myo2p Does Not Coimmunoprecipitate with Soluble Overexpressed Tail

The indirect-immunofluorescence studies described above demonstrated that the overexpressed tail localizes to sites of polarized cell growth. The overexpressed tail may localize to the bud tip via an association with full-length endogenous Myo2p or by binding to a localization determinant in the bud tip. To assess the potential for interaction between the endogenous Myo2p and the overexpressed tail, immunoprecipitation experiments were performed. Unfortunately, very little HA-tagged tail is immunoprecipitable from the 100,000 × *g* pellet fraction, presumably because the epitope is masked. However, the HA-tagged tail could be quantitatively immunoprecipitated from the 100,000 × *g* supernatant. No endogenous Myo2p coimmunoprecipitated with the HA-tagged tail from this supernatant (Figure 9). Thus, no soluble HA-tagged tail associates with the endogenous Myo2p. It remains a possibility that the HA-tagged tail found in the pellet fraction may localize via an association with the endogenous Myo2p. However, because no endogenous Myo2p is localized to the bud tip after 1 h of growth in galactose (Figure 7), it remains unlikely that tail localization is due to an association with the endogenous Myo2p.

DISCUSSION

The results presented here demonstrate that overexpression of the tail domain of Myo2p results in a dominant–negative phenotype. Conclusions drawn from this analysis are based on the assumption that the tail domain competitively disrupts interactions of the tail domain of the endogenous Myo2p that are critical for its essential functions in the cell. Two lines of evidence indicate that this is a valid assumption. First, the phenotype of *MYO2DN* is quite similar to that observed in *myo2–66* cells grown at the

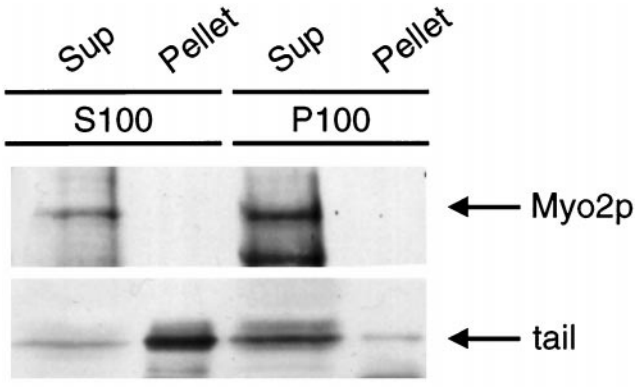

Figure 9. Endogenous Myo2p does not coimmunoprecipitate with soluble HA-tagged overexpressed tail. *MYO2DN* cells were grown in galactose for 1 h. The postnuclear supernatant was spun at 100,000 × *g* for 1 h, resulting in S100 and P100. The monoclonal anti-HA antibody, 12CA5, was used to immunoprecipitate the HA-tagged tail from both S100 and P100. The immunoprecipitated material (Pellet) and unbound material (Sup) were loaded onto SDS-PAGE gels using volumetric stoichiometry. Immunoblots were performed using anti-Myo2p motor-domain antibody (top panel) or anti-HA polyclonal antibody (lower panel).

restrictive temperature. Second, the tail domain properly localizes to the bud at early times after inducing expression, indicating that the folding state of the tail domain is sufficiently native to recognize "factors" responsible for localization. Taken together, these results strongly suggest that the effects of tail overexpression are specific and not due to general toxic effects.

There are several ways in which the presence of excess tail domain could disrupt Myo2p function. The tail domain of Myo2p may conformationally regulate motor activity (e.g., through an intramolecular, perhaps regulated, contact with the head domain, as has recently been shown for Myr3, a class I myosin; Stoffler and Bahler, 1998). The test of this hypothesis must await the purification of mechanochemically active Myo2p. Recent studies have shown that myosin-V purified from chick brain contains a tail-associated light chain also present in the tail domain of dynein (Espindola *et al.*, 1996; Benashski *et al.*, 1997). Thus, overexpression of the tail domain may disrupt Myo2p function by removing this light chain through subunit exchange. This seems unlikely, however, as the phenotype of the *slc1* (the yeast homologue of the dynein light chain) knockout does not resemble that of *myo2–66* (Dick *et al.*, 1996). This does not rule out the possibility that there are as-yet-unidentified subunits associated with the tail domain of the Myo2p heavy chain. Finally, the tail domain may disrupt the interaction of Myo2p with protein(s) and/or lipids responsible for proper subcellular localization and/or "cargo" binding. Because the tail domain can localize to the bud, and overexpression of the tail disrupts endogenous Myo2p localization, our data suggest that the tail is involved in localization.

Two reports that support our conclusions appeared while our work was in review. First, Catlett and Weisman (1998) showed that the tail domain of Myo2p is essential for function and that its deletion is lethal. Additionally, they reported the identification of a second allele of Myo2p, *myo2–2*, which contains a point mutation in the tail domain of Myo2p. This mutant disrupts association of *myo2–2* with vacuole membranes, demonstrating that the tail domain of Myo2p is important for localization to vacuole membranes. The second report showed that the tail domain of myosin Va from mouse is sufficient for localization, and overexpression of this domain mimics the *dilute* phenotype of accumulation of melanosomes in a perinuclear region of melanoctyes (Wu *et al.*, 1998).

A central conclusion to be drawn from these studies is that the tail domain is sufficient to localize Myo2p to the bud. It is possible that the tail domain is targeted to the bud as a passenger on organelles propelled to the bud by endogenous Myo2p. Several lines of evidence suggest that this simple explanation is not the case. First, the tail is localized to the bud tip after 1 h of growth in galactose-containing medium, whereas the endogenous Myo2p is not. Second, no soluble endogenous Myo2p coimmunoprecipitates with the overexpressed tail. Finally, as noted above, Myo2p localizes to the bud in the presence of Latrunculin A, indicating that movement along actin is not required for localization (Ayscough *et al.*, 1997). Thus, it is possible that the tail localizes by associating with a polarized "docking" factor located in the bud, which normally functions to retain endogenous Myo2p and its cargo in the bud. Our data suggest that such a localization determinant would be distinct from components necessary to bind Myo2p to a pelletable structure (such as an organelle), because overexpression of the tail domain does not release endogenous Myo2p from the pellet at times when endogenous Myo2p is fully delocalized by immunofluorescence.

The subcellular fractionation analysis of endogenous Myo2p provides additional insights into its association state in the cell. First, there is no Myo2p present in the fractions enriched in plasma membrane; therefore, if localization to the bud requires interaction with the plasma membrane, that interaction is readily disrupted upon lysis. The fact that Myo2p is soluble and mislocalized in spheroplasted cells suggests that some aspect of Myo2 localization does rely on the plasma membrane/cell wall. Because Sec4p is also mislocalized in spheroplasted cells (Reck-Peterson, unpublished observation), we suspect that the conditions used to spheroplast yeast cells cause general depolarization. Second, there is essentially no cytosolic Myo2p, even in cells

overexpressing the tail domain. There are a number of mechanisms that could explain why Myo2p is sedimentable. One obvious possibility is that Myo2p is sedimenting as an actomyosin complex. However, there is little detectable actin present in the 100,000 × *g* pellet (our unpublished results), and ATP does not release Myo2p from the pellet fraction. The fact that the *myo2–66* allele, which may affect motor function, does not affect pellet binding also argues against actin binding being involved in pellet association. It is possible that Myo2p is found in the 100,000 × *g* pellet because it is associated with some other large protein complex; the salt extraction data would be consistent with this possibility. Alternatively, Myo2p may be associated with vesicles that pellet at 100,000 × *g*. If this were the case, the extraction studies performed indicate that Myo2p is not simply trapped in a lumenal compartment or bound to vesicles via lipids or integral membrane proteins that would be solubilized by detergent. Rather, our data suggest that if Myo2p is bound to the surface of vesicles, it is peripherally associated with them, perhaps through a vesicle coat or proteinaceous scaffold. Future studies will focus on revealing the molecular basis for the association of Myo2p with the pellet fraction and the identity of the material that Myo2p associates with in this fraction.

Although the analysis of *MYO2DN* has been valuable for understanding Myo2p localization in the cell, it has also allowed us to temporally order *myo2* phenotypes. The earliest phenotypes detectable for *MYO2DN* are the accumulation of cytoplasmic vesicles and the mislocalization of the endogenous Myo2p. Depolarization of the yeast cell (as assayed by budding efficiency and Sec4p localization), disruption of the actin cytoskeleton, and the accumulation of Berkeley bodies are observed after longer periods of growth on galactose. It has been a formal possibility that Myo2p's role in vesicle trafficking was to organize the actin cytoskeleton (Lillie and Brown, 1994). However, because actin localization appears normal after short shifts to galactose, when vesicle accumulation can be detected, our work suggests that Myo2p may play a more direct role in vesicle trafficking.

This work provides new insights into the function of the tail domain of Myo2p, a yeast class V myosin. Using the tools generated in this study we are currently in the process of searching for proteins that may interact with the tail domain of Myo2p using both genetic and biochemical approaches. We expect that such proteins will be important for localizing the myosin within the cell, given the phenotype caused by overexpression of the tail of Myo2p.

ACKNOWLEDGMENTS

We thank the 1998 MBL Physiology course for their contributions to the characterization of the fractionation of Myo2p. We thank Tatiana Karpova for the MYO2-GFP construct. We also thank Lisa Evans, Fern Finger, Tama Hasson, Viktor Stolc, and Rania Zaarour for their many helpful suggestions and encouragement. We are grateful to many members of the Mooseker and Novick laboratories for helpful comments and review of this manuscript. This work was supported by National Institute of Health grants GM-35370 to P.J.N. and DK-25387 to M.S.M.

REFERENCES

Adams, A.E.M., and Pringle, J.R. (1984). Relationship of actin and tubulin distribution to bud growth in wild-type and morphogenetic-mutant *Saccharomyces cerevisiae*. J. Cell Biol. *98*, 934–945.

Ayscough, K.R., Stryker, J., Pokala, N., Sanders, M., Crews, P., and Drubin, D.G. (1997). High rates of actin filament turnover in budding yeast and roles for actin in establishment and maintenance of cell polarity revealed using the actin inhibitor Latrunculin-A. J. Cell Biol. *137*, 399–416.

Benashski, S.E., Harrison, A., Patel-King, R.S., and King, S.M. (1997). Dimerization of the highly conserved light chain shared by dynein and myosin V. J. Biol. Chem. *272*, 20929–20935.

Bobala, N., Jansen, R.P., Shin, T.H., and Nasmyth, K. (1996). Asymmetric accumulation of Ash1p in postanaphase nuclei depends on a myosin and restricts yeast mating-type switching to mother cells. Cell *84*, 699–709.

Brennwald, P., Kearns, B., Champion, K., Keranen, S., Bankaitis, V., and Novick, P. (1994). Sec9 is a SNAP-25-like component o f a yeast SNARE complex that may be the effector of Sec4 function in exocytosis. Cell *79*, 245–258.

Brown, S.S. (1997). Myosins in yeast. Curr. Opin. Cell Biol. *9*, 44–48.

Catlett, L.N., and Weisman, L.S. (1998). The terminal tail region of a yeast Myosin-V mediates its attachment to vacuole membranes and sites of polarized growth. Proc. Natl. Acad. Sci. USA *95*, 14799–14804.

Chant, J. (1996). Generation of cell polarity in yeast. Curr. Opin. Cell Biol. *8*, 557–565.

Chowdhury, S., Smith, K.W., and Gustin, M.C. (1992). Osmotic stress and the yeast cytoskeleton: phenotype-specific suppression of an actin mutation. J. Cell Biol. *118*, 561–571.

Chuang, J.S., and Schekman, R.W. (1996). Differential trafficking and timed localization of two chitin synthase proteins Chs2p and Chs3p. J. Cell Biol. *135*, 597–610.

Dick, T., Surana, U., and Chia, W. (1996). Molecular and genetic characterization of *SLC1*, a putative *Saccharomyces cerevisiae* homolog of the metazoan cytoplasmic dynein light chain 1. Mol. Gen. Genet. *251*, 38–43.

Espindola, F.S., Cheney, R.E., King, S.M., Suter, D.M., and Mooseker, M.S. (1996). Myosin-V and dynein share a similar light chain. Mol. Biol. Cell *7*, 372a.

Espreafico, E.M., Cheney, R.E., Matteoli, M., Nascimento, A.A., De Camilli, P.V., Larson, R.E., and Mooseker, M.S. (1992). Primary structure and cellular localization of chicken brain myosin-V (p190), an unconventional myosin with calmodulin light chains. J. Cell Biol. *119*, 1541–1557.

Evans, L.L., Hammer, J., and Bridgman, P.C. (1997). Subcellular localization of myosin V in nerve growth cones and outgrowth from dilute-lethal neurons. J. Cell Sci. *110*, 439–449.

Evans, L.L., Lee, A.J., Bridgman, P.C., and Mooseker, M.S. (1998). Vesicle-associated brain myosin-V can be activated to catalyze actin-based transport. J. Cell Sci. *111*, 2055–2066.

Finger, F., Hughes, T.E., and Novick, P. (1998). Sec3p is a spatial landmark for polarized secretion in budding yeast. Cell *92*, 559–571.

Finger, F.P., and Novick, P. (1997). Sec3p is involved in secretion and morphogenesis in *Saccharomyces cerevisiae*. Mol. Biol. Cell *8*, 647–662.

Govindan, B. (1995). Myo2 Is a Class V Myosin That Functions in postGolgi Vesicular Transport in *Saccharomyces cerevisiae*. Ph.D. Thesis. New Haven, CT: Yale University.

Govindan, B., Bowser, R., and Novick, P. (1995). The role of Myo2, a yeast class V myosin, in vesicular transport. J. Cell Biol. *128*, 1055–1068.

Griscelli, C., Durandy, A., Guy-Grand, D., Daguillard, F., Herzog, C., and Prunieras, M. (1978). A syndrome associating partial albinism and immunodeficiency. Am. J. Med. *65*, 691–702.

Haarer, B.K., Lillie, S.H., Adams, A.E.M., Magdolen, V., Bandlow, W., and Brown, S.S. (1990). Purification of profilin from *Saccharomyces cerevisiae* and analysis of profilin-deficient cells. J. Cell Biol. *110*, 105–114.

Haarer, B.K., Petzold, A., Lillie, S.H., and Brown, S.S. (1994). Identification of MYO4, a second class V myosin gene in yeast. J. Cell Sci. *107*, 1055–1064.

Heintzelman, M.B., and Schwartzman, J.D. (1997). A novel class of unconventional myosins from *Toxoplasma gondii*. J. Mol. Biol. *8*, 139–146.

Hill, K.L., Catlett, N.L., and Weisman, L.S. (1996). Actin and myosin function in directed vacuole movement during cell division in *Saccharomyces cerevisiae*. J. Cell Biol. *135*, 1535–1549.

Jagadish, M.N., and Carter, B.L.A. (1977). Genetic control of cell division in yeast cultured at different growth rates. Nature *269*, 145–147.

Jansen, R.P., Dowzer, C., Michaelis, C., Galova, M., and Nasmyth, K. (1996). Mother cell-specific HO expression in budding yeast depends on the unconventional myosin Myo4p and other cytoplasmic proteins. Cell *84*, 687–697.

Johnston, G.C., Prendergast, J.A., and Singer, R.A. (1991). The *Saccharomyces cerevisiae MYO2* gene encodes an essential myosin for vectorial transport of vesicles. J. Cell Biol. *113*, 539–551.

Kilmartin, J.V., and Adams, A.E.M. (1984). Structural rearrangements of tubulin and actin during the cell cycle of the yeast *Saccharomyces*. J. Cell Biol. *98*, 922–933.

Lillie, S.H., and Brown, S.S. (1992). Suppression of a myosin defect by a kinesin-related gene. Nature *356*, 358–361.

Lillie, S.H., and Brown, S.S. (1994). Immunofluorescence localization of the unconventional myosin, Myo2p, and the putative kinesin-related protein, Smy1p, to the same regions of polarized growth in *Saccharomyces cerevisiae*. J. Cell Biol. *125*, 825–842.

Lillie, S.H., and Brown, S.S. (1998). Smy1p, a kinesin-related protein that does not require microtubules. J. Cell Biol. *140*, 873–883.

Liu, H., and Bretscher, A. (1989). Disruption of the single tropomyosin gene in yeast results in the disappearance of actin cables from the cytoskeleton. Cell *57*, 233–242.

Liu, H., and Bretscher, A. (1992). Characterization of *TPM1* disrupted yeast cells indicates an involvement of tropomyosin in directed vesicular transport. J. Cell Biol. *118*, 285–299.

Long, R.M., Singer, R.H., Meng, X., Gonzalez, I., Nasmyth, K., and Jansen, R.P. (1997). Mating type switching in yeast controlled by asymmetric localization of *ASH1* mRNA. Science *277*, 383–387.

Mercer, J.A., Seperack, P.K., Strobel, M.C., Copeland, N.G., and Jenkins, N.A. (1991). Novel myosin heavy chain encoded by murine *dilute* coat color locus. Nature *349*, 709–713.

Mermall, V., Post, P.L., and Mooseker, M.S. (1998). Unconventional myosins in cell movement, membrane traffic, and signal transduction. Science *279*, 527–533.

Nascimento, A.A.C., Cheney, R.E., Tauhata, S.B.F., Larson, R.E., and Mooseker, M.S. (1997). Enzymatic characterization and functional domain mapping of brain myosin-V. J. Biol. Chem. *271*, 17561–17569.

Novick, P., and Botstein, D. (1985). Phenotypic analysis of temperature-sensitive yeast actin mutants. Cell *40*, 405–416.

Novick, P., and Brennwald, P. (1993). Friends and family: the role of the Rab GTPases in vesicular traffic. Cell *19*, 597–601.

Novick, P., Osmond, B.C., and Botstein, D. (1989). Suppressors of yeast actin mutations. Genetics *121*, 659–674.

Novick, P., and Zerial, M. (1997). The diversity of Rab proteins in vesicle transport. Curr. Opin. Cell Biol. *9*, 496–504.

Pastural, E., Barrat, F.J., Dufourcq-Lagelouse, R., Certain, S., Sanal, O., Jabado, N., Seger, R., Griscelli, C., Fischer, A., and de Saint Basile, G. (1997). Griscelli disease maps to chromosome 15q21 and is associated with mutations in the myosin-Va gene. Nat. Genet. *16*, 289–292.

Prekeris, R., and Terrian, D.M. (1997). Brain myosin V is a synaptic vesicle-associated motor protein: evidence for a Ca2+-dependent interaction with the synaptobrevin-synaptophysin complex. J. Cell Biol. *137*, 1589–1601.

Probst, F.J., *et al*. (1998). Correction of deafness in shaker-2 mice by an unconventional myosin in a BAC transgene. Science *280*, 1444–1447.

Provance, D.W., Jr., Wei, M., Ipe, V., and Mercer, J.A. (1996). Cultured melanocytes from dilute mutant mice exhibit dendritic morphology and altered melanosome distribution. Proc. Natl. Acad. Sci. USA *93*, 14554–14558.

Rogers, S.L., and Gelfand, V.I. (1998). Myosin cooperates with microtubule motors during organelle transport in melanophores. Curr. Biol. *8*, 161–164.

Roth, D., Guo, W., and Novick, P. (1998). Dominant negative alleles of SEC10 reveal distinct domains involved in secretion and morphogenesis in yeast. Mol. Biol. Cell *9*, 1725–1739.

Salminen, A., and Novick, P.J. (1987). A ras-like protein is required for a postGolgi event in yeast secretion. Cell *49*, 527–538.

Santos, B., and Snyder, M. (1997). Targeting of chitin synthase 3 to polarized growth sites in yeast requires Chs5p and Myo2p. J. Cell Biol. *136*, 95–110.

Stoffler, H.E., and Bahler, M. (1998). The ATPase activity of Myr3, a rat myosin I, is allosterically inhibited by its own tail domain and by Ca2+ binding to its light chain calmodulin. J. Biol. Chem. *273*, 14605–14611.

Takagishi, Y., Oda, S.-I., Hayasaka, S., Dekker-Ohno, K., Shikata, T., Inouye, M., and Yamamura, H. (1996). The *dilute-lethal* (d^l) gene attacks a Ca^{2+} store in the dendritic spine of Purkinje cells in mice. Neurosci. Lett. *215*, 169–172.

Takizawa, P.A., Sil, A., Swedlow, J.R., Herskowitz, I., and Vale, R.D. (1997). Actin-dependent localization of an RNA encoding a cell-fate determinant in yeast. Nature *389*, 90–93.

Walch-Solimena, C., Collins, R.N., and Novick, P.J. (1997). Sec2p mediates nucleotide exchange on Sec4p and is involved in polarized delivery of postGolgi vesicles. J. Cell Biol. *137*, 1495–1509.

Wang, A., *et al*. (1998). Association of unconventional myosin MYO15 mutations with human nonsyndromic deafness DFNB3. Science *280*, 1447–1451.

Wang, Y.X., Zhao, H., Harding, T.M., Gomes de Mesquita, D.S., Woldringh, C.L., Klionosky, D.J., Munn, A.L., and Weisman, L.S. (1996). Multiple classes of yeast mutants are defective in vacuole partitioning yet target vacuole proteins correctly. Mol. Biol. Cell *7*, 1375–1389.

Wu, X., Bowers, B., Rao, K., Qin, W., and Hammer, J.A., III (1998). Visualization of melanosome dynamics within wild-type and dilute melanocytes suggests a paradigm for myosin V function in vivo. J. Cell Biol. *143*, 1899–1918.

Wu, X., Bowers, B., Wei, Q., Kocher, B., and Hammer, J.A., III (1997). Myosin V associates with melanosomes in mouse melanocytes: evidence that myosin V is an organelle motor. J. Cell Sci. *110*, 847–859.